Analysis of Carrier Frequency Offset in Alamouti Space-Time-Frequency Coded OFDM Systems

Himal A. Suraweera and Jean Armstrong
Department of Electrical and Computer Systems Engineering
Monash University
Melbourne Victoria 3800, Australia
E-mail: {himal.suraweera, jean.armstrong}@eng.monash.edu.au

***Abstract*— It is well known that orthogonal frequency division multiplexing (OFDM) systems are sensitive to carrier frequency offset (CFO). In this paper we present the effects of CFO for OFDM systems where the Alamouti code is used to map adjacent subcarriers (space-frequency) or symbols (space-time) across the space-frequency grid. Simulation results show that space-time-frequency coded OFDM systems are more sensitive to CFO effects than conventional OFDM. We have also presented an analytical error performance analysis for the case of STC-OFDM over frequency flat Rayleigh fading channels. The theoretical results have been validated from the simulations. However the usually assumed signal independent Gaussian ICI analysis provides pessimistic results.**

I. Introduction

A combination of orthogonal frequency division multiplexing (OFDM) and multiple-input multiple-output (MIMO) technology is an attractive way of realizing the high bit rates required for future communication systems. MIMO-OFDM is currently in the process of been standardized for the high speed IEEE wireless LAN standard (802.11.n) and have received much research attention for implementing fourth generation mobile communication systems. OFDM systems with transmit/receive diversity can be realized by using either spatial multiplexing, space time-frequency coding or delay diversity techniques [1], [2], [3]. In space frequency coded OFDM (SFC-OFDM) redundancy is introduced by coding across the subcarriers within an OFDM symbol and symbols transmitted across several antennas.

OFDM is sensitive to intercarrier interference (ICI) due to carrier frequency offset (CFO) and Doppler shift [4-6]. Since OFDM subcarriers are closely packed compared to the system bandwidth (in DVB 2048 or 8196 subcarriers) the amount of tolerable frequency offset is a small fraction of the OFDM bandwidth [6]. CFO introduces both attenuation/rotation of the useful signal and ICI which destroys the orthogonality of demodulated subcarriers. ICI and attenuation/phase rotation effects if not compensated, increase the system error rate and reduce the overall throughput.

The existing literature on MIMO-OFDM techniques usually assumes perfect synchronization conditions. However recently some authors have addressed frequency synchronization for MIMO-OFDM and OFDM systems based on V-BLAST architecture [7]. In [8] a combined approach is presented on phase noise, CFO and channel estimation error effects for maximum ratio combined OFDM and space-time OFDM in frequency selective multipath channels. An error analysis is also reported for BPSK and QPSK modulated conventional OFDM and space time coded OFDM (STC-OFDM) in frequency flat Rayleigh fading conditions [9].

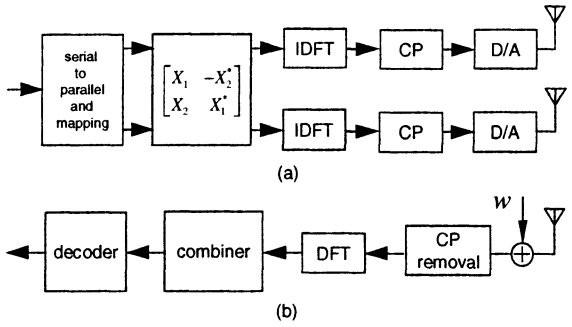

Fig. 1. Block diagram of an Alamouti coded transmit diversity OFDM system. (a) Transmitter (b) Receiver.

In this paper we investigate the impact of CFO for M-QAM modulated STC-OFDM and SFC-OFDM. It is shown that when CFO is present in SFC-OFDM both the coding structure and other subcarriers within the two OFDM symbols contribute interference. The adjacent subcarrier combining performed to obtain the decision variables introduces various interference terms.

We also show from simulations that Alamouti coded OFDM systems are more sensitive to CFO errors than conventional OFDM. The common phase error (CPE) is reduced for SFC-OFDM and STC-OFDM. An analytical symbol error rate (SER) analysis is also presented for STC-OFDM in flat Rayleigh fading channels. In space-time channels, the both the useful OFDM signal and ICI are affected by the underlying effective fading process. Hence simplifying the non-Gaussian nature of as Gaussian, but considering the fading process on ICI produces accurate theoretical results for most cases of interest. As our simulations indicate this approach deviates slightly at high signal-to-noise ratios (SNR) for a small group of ICI values. For these values the adjacent significant ICI coefficients (or the non-Gaussian characteristics) must be considered along with fading channel statistics.

The rest of the paper is organized as follows. In Section

978-3-8007-2909-8/05/$20.00 ©2005 IEEE

II and III we present the SFC-OFDM model and the impact of CFO. Section IV describes the SER analysis in frequency flat Rayleigh channels for STC-OFDM. Simulation results are presented in Section V and finally Section VI draws some conclusions.

II. Alamouti Coded SFC-OFDM Model

We consider a transmit diversity OFDM system with $n_T = 2$ transmit and $n_R = 1$ receive antennas without loss of generality [9]. At the transmitter data bits are multiplexed to the two transmit antennas, serial/parallel converted and mapped onto a modulation alphabet $\mathcal{X}$. For 4-QAM, $\mathcal{X} \in (\pm 1 \pm j)$. Consider the use of OFDM with Alamouti coding [2]. In this case there are two possible coding options. In one approach, the Alamouti code is used across space and time [10], [11]. We refer to this approach as STC-OFDM and may be impractical in fast fading conditions [10, p.186]. The requirement that the channel remains to be constant over two consecutive OFDM symbol periods may not be satisfied. For a detailed analysis of CFO effects for an STC-OFDM model we refer the interested reader to [9].

Alternatively Alamouti coding can be performed across space and frequency if the frequency domain channel coefficients are the same for two adjacent subcarriers, $H_k^{(t)} = H_{k+1}^{(t)}$ for any t [10, p.185]. So within two OFDM symbols, complex alphabet values X_1, X_2 and $-X_2^*, X_1^*$ are mapped onto the kth and $(k+1)$th subcarriers respectively. $(\cdot)^*$ denotes the complex conjugate.

$$\mathbf{X}_1 = [X_1(0), -X_2^*(1), .., X_1(N-2), -X_2^*(N-1)]^T \quad (1)$$
$$\mathbf{X}_2 = [X_2(0), X_1^*(1), .., X_2(N-2), X_1^*(N-1)]^T$$

We refer to this approach as SFC-OFDM and is used in the following description. In (1) $\mathbf{X}_1, \mathbf{X}_2$ are the transmit OFDM symbols for antenna 1 and 2. N is the total number of subcarriers. Following Alamouti mapping an inverse discrete Fourier transform (IDFT) is applied to $\mathbf{X}_1$ and $\mathbf{X}_2$ to obtain the time domain signals, a cyclic prefix P greater than the channel length is appended and the extended symbols are transmitted.

Let $\mathbf{x}(n)$ denote the discrete time $n_T \times 1$ transmitted OFDM samples $[x_1(n), x_2(n)]^T$ and $y(n)$ be the received signal. $y(n)$ is given by

$$y(n) = \sum_{l=0}^{L-1} \mathbf{h}_l \mathbf{x}(n-l) + w(n) \quad (2)$$

where $n = -P, -P+1, ..., (N-1)$. The $n_R \times n_T$ vector $\mathbf{h}_l$ represents entries from the lth tap. $\mathbf{h}_l$ contains Gaussian variables $\mathcal{CN}(0, \sigma_l^2)$, where σ_l^2 is derived from the channel power delay profile. $w(n) \backsim \mathcal{N}(0, \sigma_W^2)$ is the additive white Gaussian noise (AWGN).

The receiver detects the transmitted symbols from Y_k and Y_{k+1}. Here $k = 0, 2, \ldots, (N-2)$ and Y_k denotes the kth subcarrier received signal after DFT processing.

$$Y_k = H_{1,k} X_{1,k} + H_{2,k} X_{2,k} + W_k \quad (3)$$
$$Y_{k+1} = -H_{1,k} X_{2,k}^* + H_{2,k} X_{1,k}^* + W_{k+1}$$

where $H_{i,k}$ is the kth frequency domain channel response for the ith transmit antenna. The decision variables $\tilde{X}_1, \tilde{X}_2$ at the output of the receiver combiner is [2]

$$\tilde{X}_1 = H_{1,k}^* Y_k + H_{2,k} Y_{k+1}^* \quad (4)$$
$$\tilde{X}_2 = H_{2,k}^* Y_k - H_{1,k} Y_{k+1}^* \quad (5)$$

III. Impact of CFO for SFC-OFDM

In this Section we analyze the CFO effects for the SFC-OFDM system described. The received signal for the kth subcarrier after cyclic prefix removal and DFT processing in the presence of CFO is given by [4]

$$\begin{aligned} Y_k' &= \frac{1}{N} \sum_{n=0}^{N-1} y(n) e^{\frac{-j2\pi kn}{N}} + W_k \quad (6) \\ &= \frac{1}{N} \sum_{n=0}^{N-1} e^{\frac{j2\pi \epsilon n}{N}} \sum_{m=0}^{N-1} \mathbf{H}(m)\mathbf{X}(m) e^{\frac{j2\pi (m-k)n}{N}} + W_k \\ &= \frac{1}{N} \sum_{m=0}^{N-1} \mathbf{H}(m)\mathbf{X}(m) S_{m-k} + W_k \end{aligned}$$

where ϵ is the normalized CFO and phase offset is assumed to be zero at the beginning of the OFDM symbol. The discrete time domain OFDM signal is multiplied by $e^{j2\pi n\epsilon/N}$ in (6) to represent the CFO effect. The ICI coefficients S_k are given by

$$\begin{aligned} S_k &= \frac{1}{N} \sum_{n=0}^{N-1} e^{\frac{j2\pi n\epsilon}{N}} . e^{\frac{j2\pi kn}{N}} \quad (7) \\ &= \frac{\sin \pi(k+\epsilon)}{N \sin \frac{\pi}{N}(k+\epsilon)} \exp\left[j\pi \left(\frac{N-1}{N} \right) (k+\epsilon) \right] \end{aligned}$$

In conventional OFDM, S_0 introduces constellation "shrinkage" ($|S_0| < 1, \epsilon \neq 0$) and "rotation" [4]. The shrinkage effect is negligible for all practical values of CFO. The CPE is $\arg(S_0)$. The analysis of the effects of CFO is dependant on how the CPE is corrected at the receiver. To quantify the CFO effects, (6) is expanded for Y_k' and Y_{k+1}'.

$$\begin{aligned} Y_k' &= S_0(H_{1,k}X_1 + H_{2,k}X_2) \quad (8) \\ &\quad - S_1(H_{1,k}X_2^* - H_{2,k}X_1^*) + I_k + W_k \\ Y_{k+1}' &= S_{-1}(H_{1,k}X_1 + H_{2,k}X_2) \quad (9) \\ &\quad + S_0(-H_{1,k}X_2^* + H_{2,k}X_1^*) + I_{k+1} + W_{k+1} \end{aligned}$$

In practice the values for channel coefficients $H_{1,k}$ and $H_{2,k}$ will depend on the receiver channel estimation algorithm and pilot training employed. Some receivers will effectively output $S_0 H_{1,k}$ and $S_0 H_{2,k}$ as channel coefficients instead of $H_{1,k}$ and $H_{2,k}$. The following equations must be adjusted accordingly depending upon the channel coefficients used in (4)-(5). In the presence of CFO,

$$\begin{aligned} \tilde{X}_1' &= X_1(S_0|H_{1,k}|^2 + S_0^*|H_{2,k}|^2) \quad (10) \\ &\quad + X_1^* H_{1,k}^* H_{2,k}(S_1 + S_{-1}^*) \\ &\quad + X_2^*(S_{-1}^*|H_{2,k}|^2 - S_1|H_{1,k}|^2) + I_k' \\ &\quad + (H_{1,k}^* W_k + H_{2,k} W_{k+1}^*) \end{aligned}$$

and $\tilde{X}_2^{'}$ is given by

$$\begin{aligned}\tilde{X}_2^{'} &= X_2(S_0^*|H_{1,k}|^2 + S_0|H_{2,k}|^2) \\ &- X_2^* H_{1,k} H_{2,k}^* (S_1 + S_{-1}^*) \\ &+ X_1^*(S_1^*|H_{2,k}|^2 - S_{-1}|H_{1,k}|^2) + I_{k+1}^{'} \\ &+ (H_{2,k}^* W_k - H_{1,k} W_{k+1}^*)\end{aligned} \tag{11}$$

We have omitted the power normalization constants from (10) and (11) for equation brevity. Eqs. (10) and (11) indicate the impact of the Alamouti mapping for $\epsilon \neq 0$. CPE is reduced due to the receiver combining. In the first term of (10) or (11) $\arg\{(S_0^*|H_{1,k}|^2 + S_0|H_{2,k}|^2)\} < \arg\{S_0\}$. However since complex values X_1 and X_2 are Alamouti mapped onto adjacent subcarrier indexes k and $(k+1)$ they also appear in the useful subcarrier expressions in (10)-(11). Also ICI is introduced for the decision variables due to the loss of orthogonality among the demodulated subcarriers. I_k and I_{k+1} indicate the interference contributions from other subcarriers $(\neq k, k+1)$ for the kth and $(k+1)$th subcarriers respectively.

This analysis is slightly different from the case of STC-OFDM where Alamouti coding is performed across OFDM symbols. In STC-OFDM, since the modulated values are Alamouti mapped onto the same subcarrier over two consecutive OFDM symbols, when combining only ICI from different subcarriers interfere for the subcarrier of interest. For STC-OFDM result after combining is given by (neglecting AWGN)

$$\begin{aligned}\tilde{X}_{1,k}^{'} &= (S_0^*|H_{1,k}|^2 + S_0|H_{2,k}|^2)X_{1,k} \\ &+ H_{2,k}H_{1,k}^* X_{2,k}(S_0 - S_0^*) \\ &+ H_{1,k}^* \left(\sum_{l=0,\, l\neq k}^{N-1} a_l S_{l-k}\right) + H_{2,k}\left(\sum_{l=0,\, l\neq k}^{N-1} b_l S_{l-k}^*\right)\end{aligned} \tag{12}$$

where $a_l = H_{1,l}X_{1,l}$ and $b_l = H_{2,l}^* X_{2,l}^*$.

Fig. 2 shows the scatter diagram of a received 4-QAM constellation when Alamouti code is used. ($\epsilon = 0.02$ and 0.04). AWGN was not considered. For comparison we have presented the same for conventional OFDM. Channel coefficients were set to unity in Figs. 2-(c) and 2-(d). The scatter diagrams for OFDM show a rotation due to the CPE and cloud like ICI noise around the signal points. In SFC-OFDM, the constellation rotation is less compared to OFDM. In Fig. 2-(c) the received constellation points are surrounded with hurricane like crosses. The ICI generated as a result of combining the signals on adjacent subcarriers causes this distinctive pattern.

IV. Theoretical SER Analysis of STC-OFDM

In this section we investigate the analytical SER performance of STC-OFDM in flat Rayleigh fading channels where M-QAM is assumed for data transmission over the subcarriers. For the frequency flat Rayleigh channel model, all the post DFT detected subcarriers are affected by the same frequency domain channel coefficient. Hence we remove the index that denotes the frequency dependency from $H_{1,k}$ and $H_{2,k}$ (i.e., $H_{1,k} = H_1$ and $H_{2,k} = H_2$). The decision variable for $\tilde{X}_{1,k}^{'}$

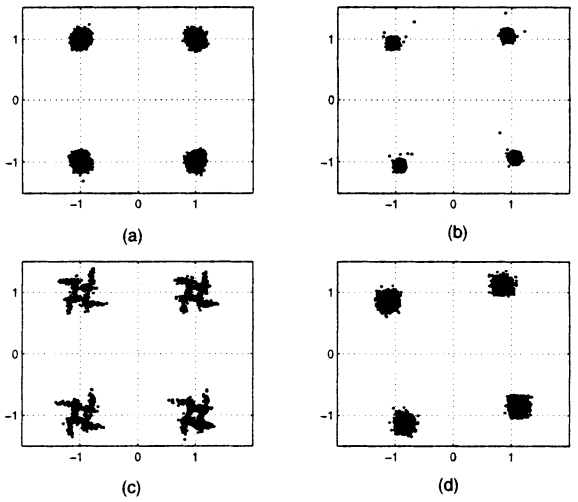

Fig. 2. Effects of CFO for Alamouti SFC-OFDM (a)-(c) and OFDM (b)-(d).

assuming perfect CPE correction is given by [9]

$$\begin{aligned}\tilde{X}_{1,k}^{'} &= |S_0|^2(|H_1|^2 + |H_2|^2)X_{1,k} \\ &+ (|H_1|^2 + |H_2|^2)S_0^*\left(\sum_{l=0,\, l\neq k}^{N-1} S_{l-k}X_{1,l}\right) \\ &+ S_0^* H_1^* W_k^t + S_0 H_2 W_k^{t+1}\end{aligned} \tag{13}$$

The instantaneous SNR γ after combining $\gamma = (|H_1|^2 + |H_2|^2)\sigma_X^2/n_T\sigma_W^2$ (neglecting ICI), is a central χ^2 random variable with 4 degrees of freedom. σ_X^2 is the average signal constellation power, $\sigma_X^2 \triangleq E(|X_k|^2)$ and $E(\cdot)$ is the expectation operator.

$$P_\gamma(\gamma) = \frac{\gamma}{\bar{\gamma}^2}\exp\left(-\frac{\gamma}{\bar{\gamma}}\right),\ \gamma \geq 0 \tag{14}$$

In (14) $\bar{\gamma} = \frac{\sigma_X^2}{n_T\sigma_W^2}$. If the ICI is considered to be Gaussian distributed then a simple expression for the resulting SER P_s is approximately given by $P_s = \int_0^\infty P_M(\gamma)P_\gamma(\gamma)d\gamma$. $P_M(\gamma)$ is modulation alphabet dependant expression for the SER and in the case of M-QAM, $P_M(\gamma)$ is expressed by [12, p.280]

$$\begin{aligned}P_M(\gamma) &= 1 - \left(1 - 2\left(1 - \frac{1}{\sqrt{M}}\right)Q\left(\sqrt{\frac{3\gamma}{M-1}}\right)\right)^2 \\ &= 4\alpha_1 Q\left(\sqrt{\alpha_2\gamma}\right)\left(1 - \alpha_1 Q\left(\sqrt{\alpha_2\gamma}\right)\right)\end{aligned} \tag{15}$$

where $\alpha_1 = (1 - 1/\sqrt{M}), \alpha_2 = 3/(M-1)$ and $Q(x) = 1/\sqrt{2\pi}\int_x^\infty e^{-t^2/2}\,dt$. By substituting (15) into P_s and simplifying we get

$$\begin{aligned}P_s(\gamma) \approx \frac{4\alpha_1}{\bar{\gamma}^2}\int_0^\infty \gamma\, Q\left(\sqrt{\frac{|S_0|^2\alpha_2\gamma}{\delta\gamma+1}}\right) \\ \times\left(1 - \alpha_1 Q\left(\sqrt{\frac{|S_0|^2\alpha_2\gamma}{\delta\gamma+1}}\right)\right)\exp\left(-\frac{\gamma}{\bar{\gamma}}\right)\,d\gamma\end{aligned} \tag{16}$$

Since the power of the received signal is preserved in the presence of CFO, (the effect of CFO is simulated using

$e^{j2\pi n\epsilon/N}$) we can simply calculate the power of the Gaussian approximated ICI term δ as

$$\delta = \sigma_X^2 \left(1 - \frac{\sin^2 \pi\epsilon}{N^2 \sin^2 \frac{\pi\epsilon}{N}}\right) \tag{17}$$

Note that (16) is different from the usually made Gaussian assumption in literature [13] where the channel attenuated ICI is considered as an independent term from the useful OFDM signal. This is referred to as "signal independent Gaussian ICI analysis" in the remainder [9]. In (16) we have averaged the faded ICI over the pdf of the effective channel χ^2 distribution. In a *faded interference channel* scenario, the SER is dominated by the "bad subcarriers" (for flat fading by a particular channel realization) where $|H_1|$ and $|H_2|$ are relatively small [14]. In these circumstances the subcarriers are least affected by the ICI. Hence the approximation of ICI as a Gaussian variable becomes increasingly accurate as we have verified this by plotting (16) with the simulated results in the next Section.

Even though (16) will result in a better SER approximation, however it does not directly consider the adjacent channel ICI coefficient correlation. Note that S_1 and S_{-1} have significant weightings over the other ICI coefficients and they have a large impact for the ICI contribution [4]. This fact can be used for a better approximation for the analytical SER derivation. This approach is beyond the scope of this paper. If the ICI is viewed as an independent interference source from the useful signal, the SER can be expressed by

$$P_s^{\mathcal{N}}(\gamma) \approx \frac{2\alpha_1}{\bar{\gamma}^2} \int_0^\infty \gamma \operatorname{erfc}\left(\sqrt{\alpha_3\gamma}\right) \times \left(1 - \frac{\alpha_1}{2}\operatorname{erfc}\left(\sqrt{\alpha_3\gamma}\right)\right) \exp\left(-\frac{\gamma}{\bar{\gamma}}\right) d\gamma \tag{18}$$

We have used $Q(x) = 0.5\ \operatorname{erfc}(x/\sqrt{2})$ and α_3 is expressed by

$$\alpha_3 = \frac{|S_0|^2\alpha_2}{2\left(\frac{\sigma_{\mathcal{N}}^2}{\sigma_W^2} + 1\right)} \tag{19}$$

The Gaussian approximated and channel independent ICI variance $\sigma_{\mathcal{N}}^2$ is calculated by

$$\sigma_{\mathcal{N}}^2 = E\left(\left|\left(\sum_{l=0,\, l\neq k}^{N-1} (|H_1|^2 + |H_2|^2) S_{l-k} X_{1,l}\right)\right|^2\right) \tag{20}$$

The expectation in (20) is obtained with respect to the channel realizations and the complex modulated values. Let $u = \operatorname{erfc}(\sqrt{\alpha_3 x})$, $dv = \frac{\gamma}{\bar{\gamma}^2}\exp(-\gamma/\bar{\gamma})$ and using the results for the CDF of the χ^2 distribution in [12] and an integral identity (eq. 3.461-2) in [15], the first integral I_1 is simplified as

$$I_1 = \frac{2\alpha_1}{\bar{\gamma}^2} \int_0^\infty \gamma \operatorname{erfc}(\sqrt{\alpha_3\gamma}) \exp\left(-\frac{\gamma}{\bar{\gamma}}\right) d\gamma \tag{21}$$
$$= 2\alpha_1 \left(1 - \sqrt{\frac{\alpha_3}{\pi}} \left(\sum_{n=0}^{1} \frac{\left(\alpha_3 + \frac{1}{\bar{\gamma}}\right)^{-(n+\frac{1}{2})} \Gamma(n+\frac{1}{2})}{\bar{\gamma}^n\, \Gamma(n+1)}\right)\right)$$

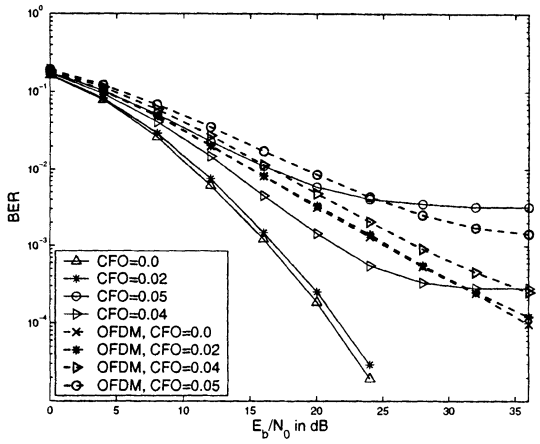

Fig. 3. BER versus E_b/N_0 for SFC-OFDM. 16-QAM and $N = 512$.

where the Gamma function $\Gamma(x) = \int_0^\infty t^{x-1}e^{-t}\ dt$. The second integral I_2 can also be analytically evaluated similarly.

$$I_2 = \frac{\alpha_1}{\bar{\gamma}^2} \int_0^\infty \gamma \operatorname{erfc}^2(\sqrt{\alpha_3\gamma}) \exp\left(-\frac{\gamma}{\bar{\gamma}}\right) d\gamma \tag{22}$$
$$= \alpha_4 \int_0^\infty (1 - e^{-\frac{\gamma}{\bar{\gamma}}} - \frac{\gamma}{\bar{\gamma}} e^{-\frac{\gamma}{\bar{\gamma}}}) \frac{e^{-\alpha_3\gamma}}{\sqrt{\gamma}} \operatorname{erfc}(\sqrt{\alpha_3\gamma})\, d\gamma$$

In (22), $\alpha_4 = 2\alpha_1\sqrt{\frac{\alpha_3}{\pi}}$. Let $z = \sqrt{\alpha_3\gamma}$ and using a series expansion for the $\operatorname{erfc}(x)$ given by

$$\operatorname{erfc}(x) = 1 - \frac{2}{\pi} e^{-x^2} \sum_{n=0}^{\infty} \frac{(-1)^n}{(2n+1)n!} x^{2n+1} \tag{23}$$

and I_2 is further simplified as

$$I_2 = \alpha_1 \left(1 - \sqrt{\frac{1}{\pi^2(1 + \frac{1}{\alpha_3\bar{\gamma}})}} \arctan\left(\sqrt{1 + \frac{1}{\alpha_3\bar{\gamma}}}\right) - \frac{1}{4\alpha_3\bar{\gamma}(1 + \frac{1}{\bar{\gamma}\alpha_3})^{\frac{3}{2}}} + \frac{1}{\pi\alpha_3\bar{\gamma}} \sum_{n=0}^{\infty} (-1)^n \frac{n}{(2n+1)(2 + \frac{1}{\alpha_3\bar{\gamma}})^{n+2}}\right) \tag{24}$$

Hence $I_1 + I_2$ gives the analytical SER. For all practical computations, the infinite summation in (24) can be truncated.

V. Simulation Results

In this Section we provide simulation and analytical results for the error performance of Alamouti coded SFC-OFDM and STC-OFDM due to CFO. A uniform power delay profile with $L = 3$ was assumed. For the simulations, $N = 512$. This guarantees that the adjacent subcarrier channel coefficients are approximately same with negligible system degradation [3]. Fig. 3 shows the BER of SFC-OFDM and conventional OFDM. As seen from Fig. 3 SFC-OFDM shows a low BER ($\epsilon \leq 0.03$) over OFDM. This is due to the diversity advantage of the former. However for $\epsilon \geq 0.04$, SFC-OFDM shows an error floor. Fig. 3 also indicates that space-time OFDM is more sensitive to CFO than OFDM. This is because although

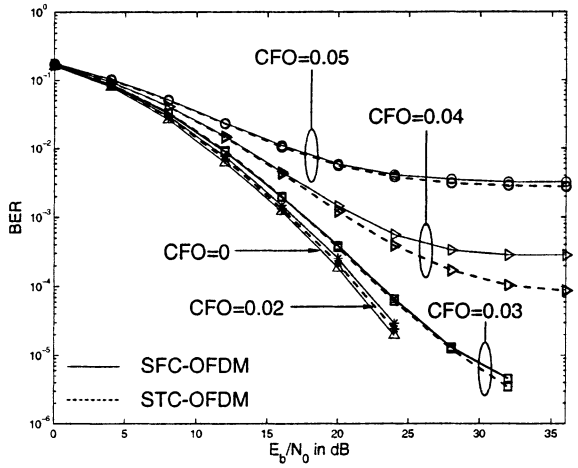

Fig. 4. BER versus E_b/N_0 for SFC-OFDM and STC-OFDM.

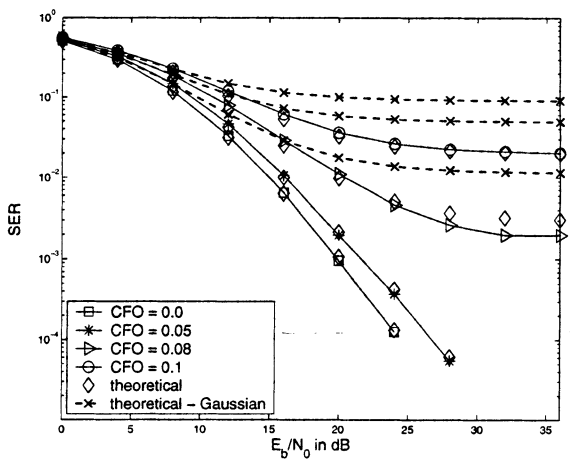

Fig. 5. SER for STC-OFDM in flat Rayleigh fading channels. 16-QAM.

compared to OFDM, SFC-OFDM is robust against fading, the channel attenuated ICI also becomes more resilient. Hence although for small CFO space-frequency OFDM shows better performance, for increasing CFO the BER gets worse. In fact at high E_b/N_0 and $\epsilon \geq 0.04$ OFDM shows a better performance.

Fig. 4 shows a BER comparison of STC-OFDM and SFC-OFDM in the same frequency selective fading channel. The channel is block fading but remains constant over two consecutive OFDM symbol periods as required by STC-OFDM. Although both the systems exhibit similar error performance for $\epsilon = 0.04$, STC-OFDM clearly shows a better performance. The reasoning behind this observation could be explained based on the different ICI structures, the two systems have.

The analytical and simulated results for STC-OFDM in a frequency flat fading scenario are shown in Fig. 5. $N = 64$. We have evaluated (16) using Monte Carlo integration. Although ICI is approximated as Gaussian, the theoretical results match with the simulations precisely for all CFOs except for $\epsilon = 0.08$ where they deviate slightly at high E_b/N_0. This is due to considering the fading effects on ICI in (16). For $\epsilon = 0.08$ we could consider the adjacent subcarrier ICI characteristics for an exact solution. However the analytical results using the signal independent ICI approach, of (21) and (24) deviates from the simulated results considerably. The signal independent Gaussian approximated ICI analysis has the main drawback of not considering the possible channel correlation among the ICI terms and the useful OFDM signal [9].

VI. Conclusions

In this paper we have analyzed CFO effects for Alamouti coded OFDM systems. Orthogonality among the demodulated subcarriers is lost and the receiver combining introduces additional interference terms for the decision variables. However the CPE is reduced. Simulation results showed that STC-OFDM and SFC-OFDM systems are more sensitive to CFO errors compared to conventional OFDM. This is because the channel faded ICI is also significant in the case of space-time OFDM. We also provided a theoretical SER analysis for STC-OFDM over flat fading channels, and the results closely agree with the simulations. The usually assumed signal independent Gaussian ICI method exhibits highly pessimistic results for all the CFO values considered.

References

[1] A. F. Molisch *et al.*, "Space-time-frequency (STF) coding for MIMO-OFDM systems," *IEEE Commun. Lett.*, vol. 6, pp. 370-372, Sept. 2002.

[2] B. Vucetic and J. Yuan, *Space-Time Coding*. Chichester, UK: Wiley, 2003.

[3] Y. Gong and K. B. Letaief, "An efficient space-frequency coded OFDM system for broadband wireless communications," *IEEE Trans. Commun.*, vol. 51, pp. 2019-2029, Nov. 2003.

[4] J. Armstrong, "Analysis of new and existing methods for reducing intercarrier interference due to carrier frequency offset in OFDM," *IEEE Trans. Commun.*, vol. 47, pp. 365-369, Mar. 1999.

[5] J. Armstrong *et al.*, "Polynomial cancellation coding of OFDM to reduce the intercarrier interference due to Doppler spread," in *Proc. IEEE GLOBECOM 98*, Sydney, Australia, Nov. 1998, pp. 2771-2776.

[6] P. Moose, "A technique for orthogonal frequency division multiplexing frequency offset correction," *IEEE Trans. Commun.*, vol. 42, pp. 2908-2914, Oct. 1994.

[7] A. van Zelst and Tim C. W. Schenk, "Implementation of a MIMO OFDM-based wireless LAN system," *IEEE Trans. Signal Processing*, vol. 52, pp. 483-493, Feb. 2004.

[8] R. Narasimhan, "Performance of diversity schemes for OFDM systems with frequency offset, phase noise, and channel estimation errors," *IEEE Trans. Commun.*, vol. 50, pp. 1561-1565, Oct. 2002.

[9] K. Sathananthan and C. R. N. Athaudage, "Exact probability of error of ST-coded OFDM systems with frequency offset in flat fading Rayleigh fading channels," in *Proc. Australian Communications Theory Workshop (AusCTW 2005)*, Brisbane, Australia, Feb. 2005, pp. 20-25.

[10] A. Paulraj, R. Nabar and D. Gore, *Introduction to Space-Time Wireless Communications*. Cambridge: UK, Cambridge University Press, 2003.

[11] H.-K. Song, S.-J. Kang. M.-J. Kim and Y.-H. You, "Error performance analysis of STBC-OFDM systems with parameter imbalances," *IEEE Trans. Broadcast.*, vol. 50, pp. 76-82, Mar. 2004.

[12] J. G. Proakis, *Digital Communications*. 3rd ed., New York: McGraw-Hill, 1995.

[13] X. Wang *et al.*, "SER performance evaluation and optimization of OFDM system with residual frequency and timing offsets from imperfect synchronization," *IEEE Trans. Broadcast.*, vol. 49, pp. 170-176, June 2003.

[14] K. R. Panta and J. Armstrong, "Effects of clipping on the error performance of OFDM in frequency selective fading channels," *IEEE Trans. Wireless Commun.*, vol. 3, pp. 668-671, Mar. 2004.

[15] I. S. Gradshteyn and I. M. Ryzhik, *Table of Integrals, Series, and Products*. New York, USA: Academic Press Inc., 1980.